

Cluster computations in mesoscopic wave turbulence

Miguel D. Bustamante[†] and Elena Kartashova^{*}

[†] *Mathematics Institute, University of Warwick, Coventry CV4 7AL, UK*

^{*} *RISC, J.Kepler University, Linz 4040, Austria*

Mesoscopic wave turbulence is characterized by the co-existence of two turbulent regimes: stochastic wave interactions, described by wave kinetic equations, and independent clusters of resonantly interacting waves, described by a few low-dimensional dynamical systems. We show that 1) most frequently met clusters are integrable, and 2) construction of clusters can be used as the base for the Clipping method, substantially more effective for these systems than Galerkin method. The results can be used directly for arbitrary 3-wave resonant systems.

1. Introduction. Euler equations, regarded with various boundary conditions and specific values of some parameters, describe an enormous number of nonlinear dispersive wave systems (capillary waves, surface water waves, atmospheric planetary waves, drift waves in plasma, etc.) This class of nonlinear dispersive waves can be described by the Hamiltonian equation of motion in the Fourier space [1],

$$i\dot{a}_{\mathbf{k}} = \partial\mathcal{H}/\partial a_{\mathbf{k}}^*, \quad (1)$$

where $a_{\mathbf{k}}$ is the amplitude of the Fourier mode corresponding to the wavevector \mathbf{k} and the Hamiltonian \mathcal{H} is represented as an expansion in powers \mathcal{H}_j which are proportional to the product of j amplitudes $a_{\mathbf{k}}$. In this Letter we are going to consider expansions of Hamiltonians up to third order in wave amplitude, i.e. a cubic Hamiltonian of the form

$$\mathcal{H}_3 = \sum_{\mathbf{k}_1, \mathbf{k}_2, \mathbf{k}_3} V_{23}^1 a_1^* a_2 a_3 \delta_{23}^1 + \text{complex conj.},$$

where for brevity we introduced notations $a_j \equiv a_{\mathbf{k}_j}$ and $\delta_{23}^1 \equiv \delta(\mathbf{k}_1 - \mathbf{k}_2 - \mathbf{k}_3)$ is the Kronecker symbol. If $\mathcal{H}_3 \neq 0$, three-wave process is dominant and the main contribution to the nonlinear evolution comes from the waves satisfying the following resonance conditions:

$$\begin{cases} \omega(\mathbf{k}_1) + \omega(\mathbf{k}_2) - \omega(\mathbf{k}_3) = \Omega, \\ \mathbf{k}_1 + \mathbf{k}_2 - \mathbf{k}_3 = 0, \end{cases}$$

where $\omega(\mathbf{k})$ is a dispersion relation for the linear wave frequency and $\Omega \geq 0$ is called resonance width.

If $\Omega > 0$, the equation of motion (1) turns into

$$i\dot{A}_{\mathbf{k}} = \omega_{\mathbf{k}} A_{\mathbf{k}} + \sum_{\mathbf{k}_1, \mathbf{k}_2} V_{12}^{\mathbf{k}} A_1 A_2 \delta_{12}^{\mathbf{k}} + 2V_{\mathbf{k}2}^{1*} A_1 A_2^* \delta_{\mathbf{k}2}^1. \quad (2)$$

If $\Omega = 0$, the equation of motion (1) turns into

$$i\dot{B}_{\mathbf{k}} = \sum_{\mathbf{k}_1, \mathbf{k}_2} (V_{12}^{\mathbf{k}} B_1 B_2 \delta_{12}^{\mathbf{k}} \delta(\omega_{\mathbf{k}} - \omega_1 - \omega_2) + 2V_{\mathbf{k}2}^{1*} B_1 B_2^* \delta_{\mathbf{k}2}^1 \delta(\omega_1 - \omega_{\mathbf{k}} - \omega_2)). \quad (3)$$

The co-existence of these two substantially different “layers” of wave turbulence, described by Eqs.(2) and (3), has been observed in numerical simulations [2] and proven analytically in the frame of the kinematic two-layer model of laminated turbulence [3]. Dynamics of the layer (2) is described by wave kinetic equations and is well studied

[1]. Dynamics of the layer (3) is practically not studied though a lot of preliminary results is already known. Namely, the layer (3) is described by a few independent wave clusters formed by the waves which are in exact nonlinear resonance [4]. The corresponding solutions of (2) can be computed by specially developed algorithms [5], dynamical systems describing resonant clusters can also be found algorithmically [6], as well as coefficients of dynamical systems [7]. Moreover, as it was demonstrated in [13] (numerically), [8] (analytically), these clusters “survive” for small enough but non-zero Ω . Two main goals of this Letter are: i) to study dynamics of the most frequently met resonant clusters, and ii) to show how to use resonance clusters to *simplify drastically* numerical simulations with corresponding Hamiltonian systems.

2. Clusters. In this Letter we present some analytical and numerical results for 3 most commonly met dynamical systems corresponding to non-isomorphic clusters of nonlinear resonances - a *triad*, a *kite*, and a *butterfly* consisting of 3, 4 and 5 complex variables correspondingly.

Dynamical system for a *triad* has the form

$$\dot{B}_1 = Z B_2^* B_3, \quad \dot{B}_2 = Z B_1^* B_3, \quad \dot{B}_3 = -Z B_1 B_2. \quad (4)$$

A *kite* consists of two triads *a* and *b*, with wave amplitudes B_{ja} , B_{jb} , $j = 1, 2, 3$, connected *via* two common modes. Analogously to [9], one can point out 4 types of kites according to the properties of connecting modes. For our considerations, this is not important: the general method to study integrability of kites will be the same. For the concreteness of presentation, in this Letter a *kite* with $B_{1a} = B_{1b}$ and $B_{2a} = B_{2b}$ has been chosen:

$$\begin{cases} \dot{B}_{1a} = B_{2a}^* (Z_a B_{3a} + Z_b B_{3b}), \\ \dot{B}_{2a} = B_{1a}^* (Z_a B_{3a} + Z_b B_{3b}), \\ \dot{B}_{3a} = -Z_a B_{1a} B_{2a}, \quad \dot{B}_{3b} = -Z_b B_{1a} B_{2a}. \end{cases} \quad (5)$$

A *butterfly* consists of two triads *a* and *b*, with wave amplitudes B_{ja} , B_{jb} , $j = 1, 2, 3$, connected *via* one common mode. As it was shown in [9], there exist 3 different types of butterflies, according to the choice of the connecting mode. Let us take, for instance, $B_{1a} = B_{1b} (\equiv B_1)$. The corresponding dynamical system is then

as follows:

$$\begin{cases} \dot{B}_1 = Z_a B_{2a}^* B_{3a} + Z_b B_{2b}^* B_{3b}, \\ \dot{B}_{2a} = Z_a B_1^* B_{3a}, \quad \dot{B}_{2b} = Z_b B_1^* B_{3b}, \\ \dot{B}_{3a} = -Z_a B_1 B_{2a}, \quad \dot{B}_{3b} = -Z_b B_1 B_{2b}. \end{cases} \quad (6)$$

3. Integrability of resonance clusters. Consider a general N -dimensional system of autonomous evolution equations of the form:

$$\frac{dx^i}{dt}(t) = \Delta^i(x^j(t)), \quad i = 1, \dots, N. \quad (7)$$

Any scalar function $f(x^i, t)$ that satisfies $\frac{d}{dt}(f(x^i(t), t)) = 0$ is called a *dynamical invariant* for this system. If the dynamical invariant is a scalar function of the particular form $f(x^i)$, i.e. it does not depend on time, it is called a *conservation law* (CL). We say that Sys.(7) is *integrable* if there are N functionally independent dynamical invariants. Obviously, if Sys.(7) possesses $(N - 1)$ functionally independent CLs, then it is constrained to move along a 1-dimensional manifold, and the way it moves is dictated by 1 dynamical invariant. This dynamical invariant can be obtained from the knowledge of the $(N - 1)$ CLs and the explicit form of the Sys.(7), i.e. Sys.(7) is integrable then. It follows from the Theorem below that in many cases the knowledge of only $(N - 2)$ CLs is enough for the integrability of the Sys.(7). We use hereafter Einstein convention on repeated indices and $f_{,i} \equiv \partial f / \partial x^i$.

Theorem *Let us assume that the system (7) possesses a standard Liouville volume density*

$$\rho(x^i) : (\rho \Delta^i)_{,i} = 0,$$

and $(N - 2)$ functionally independent CLs, H^1, \dots, H^{N-2} . Then a new CL can be constructed, which is functionally independent of the original ones, and therefore the system is integrable.

The (lengthy) proof follows from the existence of a Poisson bracket for the original Sys.(7) and is extension of the general approach used in [10] for three dimensional first order autonomous equations. The proof is constructive and allows us to find the explicit form of a new CL for dynamical systems of the form (4),(5),(6), etc.

Integrability of a *triad*, dynamical system (4), is a well-known fact (e.g. [11]) and its two conservation laws are

$$I_{23} = |B_2|^2 + |B_3|^2, \quad I_{13} = |B_1|^2 + |B_3|^2.$$

Sys.(4) has been used for a preliminary check of our method; in this case $N = 4$ (after elimination of the so-called slave phases). The method can thus be applied and we obtain the following CL:

$$I_T = \text{Im}(B_1 B_2 B_3^*),$$

together with the time-dependent dynamical invariant of the form:

$$S_0 = Z t - \frac{F\left(\arcsin\left(\left(\frac{R_3 - v}{R_3 - R_2}\right)^{1/2}\right), \left(\frac{R_3 - R_2}{R_3 - R_1}\right)^{1/2}\right)}{2^{1/2}(R_3 - R_1)^{1/2}(I_{13}^2 - I_{13}I_{23} + I_{23}^2)^{1/4}}.$$

Here F is the elliptic integral of the first kind, $R_1 < R_2 < R_3$ are the three real roots of the polynomial

$$x^3 + x^2 = 2/27 - (27I_T^2 -$$

$$(I_{13} + I_{23})(I_{13} - 2I_{23})(I_{23} - 2I_{13}))/27(I_{13}^2 - I_{13}I_{23} + I_{23}^2)^{3/2}$$

and

$$v = |B_1|^2 - (2I_{13} - I_{23} + (I_{13}^2 - I_{13}I_{23} + I_{23}^2)^{1/2})/3$$

is always within the interval $[R_2, R_3] \ni 0$.

A *kite*, dynamic system (5), is also an integrable system. Indeed, after reduction of slave variables the system corresponds to $N = 6$ and has 5 CLs (2 linear, 2 quadratic, 1 cubic):

$$\begin{cases} L_R = \text{Re}(Z_b B_{3a} - Z_a B_{3b}), \quad L_I = \text{Im}(Z_b B_{3a} - Z_a B_{3b}), \\ I_{1ab} = |B_{1a}|^2 + |B_{3a}|^2 + |B_{3b}|^2, \\ I_{2ab} = |B_{2a}|^2 + |B_{3a}|^2 + |B_{3b}|^2, \\ I_K = \text{Im}(B_{1a} B_{2a} (Z_a B_{3a}^* + Z_b B_{3b}^*)), \end{cases}$$

with a dynamical invariant that is essentially the same as for a triad, S_0 , after replacing $Z = Z_a + Z_b$, $I_T = I_K(Z_a^2 + Z_b^2)/Z^3$, $I_{13} = I_{1ab}(Z_a^2 + Z_b^2)/Z^2 - (L_R^2 + L_I^2)/Z^2$, $I_{23} = I_{2ab}(Z_a^2 + Z_b^2)/Z^2 - (L_R^2 + L_I^2)/Z^2$.

Dynamics of a *butterfly* is governed by the Sys.(6) and its 4 CLs (3 quadratic and 1 cubic) can easily be obtained:

$$\begin{cases} I_{23a} = |B_{2a}|^2 + |B_{3a}|^2, \quad I_{23b} = |B_{2b}|^2 + |B_{3b}|^2, \\ I_{ab} = |B_1|^2 + |B_{3a}|^2 + |B_{3b}|^2, \\ I_0 = \text{Im}(Z_a B_1 B_{2a} B_{3a}^* + Z_b B_1 B_{2b} B_{3b}^*), \end{cases} \quad (8)$$

while a Liouville volume density is $\rho = 1$. Notice that all cubic CLs are canonical Hamiltonians for the respective *triad*, *kite* and *butterfly* systems. From now on we consider the *butterfly* case when no amplitude is identically zero; otherwise the system would become integrable.

The use of standard amplitude-phase representation $B_j = C_j \exp(i\theta_j)$ of the complex amplitudes B_j in terms of real amplitudes C_j and phases θ_j shows immediately that only two phase combinations are important:

$$\varphi_a = \theta_{1a} + \theta_{2a} - \theta_{3a}, \quad \varphi_b = \theta_{1b} + \theta_{2b} - \theta_{3b},$$

a - and b -triad phases (with the requirement $\theta_{1a} = \theta_{1b}$ which correspond to the chosen resonance condition). This reduces five complex equations (6) to only four real ones:

$$\frac{dC_{3a}}{dt} = -Z_a C_1 C_{2a} \cos \varphi_a, \quad (9)$$

$$\frac{dC_{3b}}{dt} = -Z_b C_1 C_{2b} \cos \varphi_b, \quad (10)$$

$$\frac{d\varphi_a}{dt} = Z_a C_1 \left(\frac{C_{2a}}{C_{3a}} - \frac{C_{3a}}{C_{2a}} \right) \sin \varphi_a - \frac{I_0}{(C_1)^2}, \quad (11)$$

$$\frac{d\varphi_b}{dt} = Z_b C_1 \left(\frac{C_{2b}}{C_{3b}} - \frac{C_{3b}}{C_{2b}} \right) \sin \varphi_b - \frac{I_0}{(C_1)^2}. \quad (12)$$

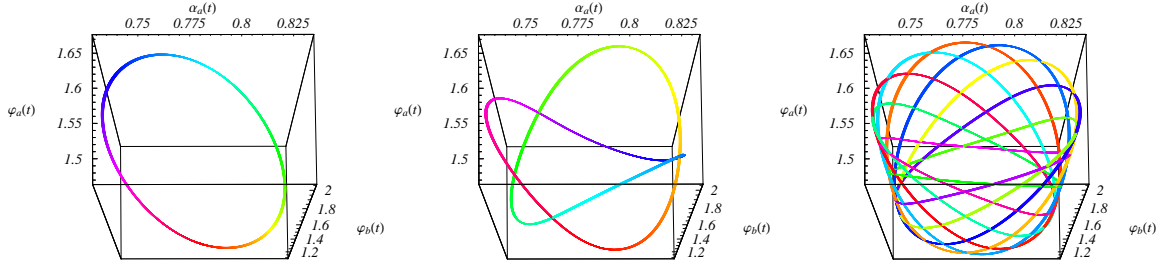


FIG. 1: Color online. To facilitate view, color hue of the plot is a linear function of time t , varying from 0 to 1 as t runs through one period. **Left panel:** $Z_a = Z_b = 10/100$, $I_{ab} \approx 2.1608$. **Middle panel:** $Z_a = 8/100$, $Z_b = 12/100$, $I_{ab} \approx 2.2088$. **Right panel:** $Z_a = 9/100$, $Z_b = 11/100$, $I_{ab} \approx 2.1846$.

The cubic CL reads

$$I_0 = C_1 (Z_a C_{2a} C_{3a} \sin \varphi_a + Z_b C_{2b} C_{3b} \sin \varphi_b) \quad (13)$$

in terms of the amplitudes and phases. This means that the dynamics of a butterfly cluster is, in the generic case, confined to a 3-dimensional manifold. Below we regard a few particular cases in which Sys.(6) is integrable.

Example 1: Real amplitudes, $\varphi_a = \varphi_b = 0$. In this case the Hamiltonian I_0 becomes identically zero while Liouville density in coordinates C_{3a}, C_{3b} is $\rho(C_{3a}, C_{3b}) = 1/C_1 C_{2a} C_{2b}$. So in this case the equations for the unknown CL $H(C_{3a}, C_{3b})$ are:

$$\rho \Delta^{C_{3a}} = -\frac{Z_a}{C_{2b}} = \frac{\partial}{\partial C_{3b}} H, \quad \rho \Delta^{C_{3b}} = -\frac{Z_b}{C_{2a}} = -\frac{\partial}{\partial C_{3a}} H,$$

and from Eqs.(8) we readily obtain

$$H(C_{3a}, C_{3b}) = Z_b \arctan(C_{3a}/C_{2a}) - Z_a \arctan(C_{3b}/C_{2b}),$$

i.e. Sys.(6) is integrable in this case. Of course, this case is degenerate for $I_0 \equiv 0$ yields no constraint on the remaining independent variables C_{3a}, C_{3b} satisfying equations (9), (10).

General change of coordinates. Going back to Eqs.(9)–(13), we can jump from this degenerate case to a more generic case by defining new coordinates which are suggested by $H(C_{3a}, C_{3b})$. The new coordinates are to replace the amplitudes C_{3a}, C_{3b} :

$$\alpha_a = \arctan(C_{3a}/C_{2a}), \quad \alpha_b = \arctan(C_{3b}/C_{2b}).$$

We choose the inverse transformation to be

$$\begin{cases} C_{2a} = \sqrt{I_{23a}} \cos(\alpha_a), & C_{3a} = \sqrt{I_{23a}} \sin(\alpha_a), \\ C_{2b} = \sqrt{I_{23b}} \cos(\alpha_b), & C_{3b} = \sqrt{I_{23b}} \sin(\alpha_b), \end{cases} \quad (14)$$

so that the domain for the new variables is $0 < \alpha_a < \pi/2$, $0 < \alpha_b < \pi/2$. For these new coordinates, the evolution equations simplify enormously:

$$\begin{cases} \frac{d\alpha_a}{dt} = -Z_a C_1 \cos \varphi_a, & \frac{d\alpha_b}{dt} = -Z_b C_1 \cos \varphi_b, \\ \frac{d\varphi_a}{dt} = Z_a C_1 (\cot \alpha_a - \tan \alpha_a) \sin \varphi_a - \frac{I_0}{(C_1)^2}, \\ \frac{d\varphi_b}{dt} = Z_b C_1 (\cot \alpha_b - \tan \alpha_b) \sin \varphi_b - \frac{I_0}{(C_1)^2}, \end{cases} \quad (15)$$

where the amplitude $C_1 > 0$ is obtained using eqs.(8):

$$C_1 = \sqrt{I_{ab} - I_{23a} \sin^2 \alpha_a - I_{23b} \sin^2 \alpha_b} \quad (16)$$

and the cubic CL is now

$$I_0 = \frac{C_1}{2} (Z_a I_{23a} \sin(2\alpha_a) \sin(\varphi_a) + Z_b I_{23b} \sin(2\alpha_b) \sin(\varphi_b)). \quad (17)$$

Equations (15)–(17) represent the final form of our 3-dimensional general system.

Example 2: Complex amplitudes, $I_0 = 0$. Here, we just impose the condition $I_0 = 0$ but the phases are otherwise arbitrary: this case is therefore not degenerate anymore and we have a 3-dimensional system which, in order to be integrable, requires the existence of only 1 CL, for instance, $A_a = \sin(2\alpha_a) \sin(\varphi_a)$, which can be deduced from Eqs.(15),(11). Making use of the Theorem, one can find another CL for this case: $H_{new}(C_{3a}, C_{3b}) = (1 + Z_b/Z_a) \arccos\left(\frac{\cos 2\alpha_a}{\sqrt{1-A_a^2}}\right) - (1 + Z_a/Z_b) \arccos\left(\frac{\cos 2\alpha_b}{\sqrt{1-A_b^2}}\right)$. Obviously A_a and H_{new} are functionally independent, i.e. the case $I_0 = 0$ is integrable.

Example 3: Complex amplitudes, $Z_a = Z_b$. In this case a new CL has the form

$$\begin{aligned} \frac{I_0^2}{Z_a} E &= C_{2a}^2 C_{3a}^2 + C_{2b}^2 C_{3b}^2 + 2C_{2a} C_{3a} C_{2b} C_{3b} \cos(\varphi_a - \varphi_b) \\ &\quad - C_1^2 (C_1^2 - C_{2a}^2 + C_{3a}^2 - C_{2b}^2 + C_{3b}^2), \end{aligned} \quad (18)$$

which is functionally independent of the other known constants of motion. Therefore, according to the Theorem the case $Z_b = Z_a$ is integrable.

4. Numerical simulations. To investigate the general behavior of a butterfly cluster with $Z_a \neq Z_b$, we integrated directly Eqs.(15),(16) with I_0 computed from Eq.(17) evaluated at $t = 0$ and used to check numerical scheme afterwards. Some results of the simulations with Sys.(15) are presented in Fig.1. Initial conditions $\alpha_a(0) = 78/100$, $\alpha_b(0) = 60/100$, $\varphi_a(0) = 147/100$, $\varphi_b(0) = 127/100$ and values of the constants of motion $I_0 = 11/2000$, $I_{23a} = 4/100$, $I_{23b} = 4/100$ are the same for all three parts of Fig.1. 3D parametric plots

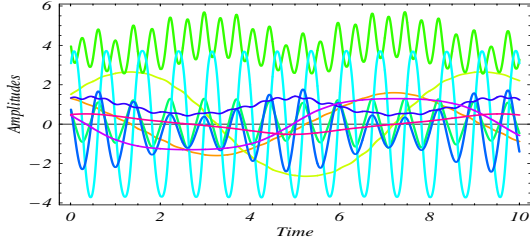


FIG. 2: Color online. Chain of 4 triads, real amplitudes for all 9 modes. Time and amplitudes in non-dimensioned units.

are shown in space $(\alpha_a, \varphi_a, \varphi_b)$ with color hue depending on time, so the plots are effectively 4D. The main goal of this series of numerical simulations was to study changes in the dynamics of a butterfly cluster according to the magnitude of the ratio $\zeta = Z_a/Z_b$. In Fig.1, left panel $\zeta_l = 1$, middle panel $\zeta_m = 2/3$ and right panel $\zeta_r = 9/11$. As it was shown above, the case $\zeta_l = 1$ is integrable, and one can see the closed trajectory with period $T_l \approx 21.7$. Quite unexpectedly, rational ζ_m, ζ_r produce what appear to be periodic motions and closed trajectories with periods $T_m \approx 53$ and $T_r \approx 215$ correspondingly. A few dozen of simulations made with different rational ratios $\zeta = Z_a/Z_b$ show that periodicity depends - or is even defined by - the commensurability of the coefficients Z_a and Z_b . Fig.1 shows that $\zeta_m = 2/3$ gives 2 spikes in one direction and 3 spikes in the perpendicular direction, while $\zeta_r = 9/11$ gives 9 and 11 spikes correspondingly; and so on. This does not mean, of course, that in the general case $Z_a \neq Z_b$ solutions of Sys.(6) are periodic. But the opposite can only be proven analytically for in numerical simulations any choice of the ratio ζ necessarily turns into a rational number.

Some preliminary series of simulations have been performed with the chains of triads with connection types as in (6), with maximum number of triads in a chain being 8 (corresponds to 17 modes). For our numerical simulations, resonant clusters of spherical Rossby waves were taken, with initial (non-dimensioned) energies of the order of measured atmospheric data, as in [12]. The dynamical system for computations was taken in the original variables B_j . The case of real amplitudes is shown in Fig.2: all resonant modes behave (almost) periodically. Non-dimensioned units for time and amplitudes were chosen to illustrate clearly the characteristic behavior of the amplitudes. The same behavior of the smallest possible clusters - triads - was observed in [13], Fig.1, in the numerical simulations with spectral model of the barotropic vorticity equation (221 modes were excited, among them 39 resonant). As for non-resonant modes, they do not change their energies at the same time scale ([13], Fig.3). Another example can be found in [6] (ocean planetary motions, 128 resonant modes among 2500 Fourier harmonics in the chosen spectral domain, all clusters and their dynamical systems are written out explicitly). In dozens of studied 3-wave systems, the amount of resonant

modes does not exceed 20% of all modes in the spectral domain.

5. Conclusions:

- i) Our analysis is based on the general structure of the dynamical systems: the results can be used directly for arbitrary 3-wave resonant system.
- ii) The idea of Clipping method (CM) - to clip out the resonant modes from the general Sys.(3) - was formulated in [14] but computer methods [5] were not known yet. CM has two advantages compared to Galerkin method (GM):
 - ii,a) The truncation of a numerical scheme in CM can be made substantially further than in GM, depending not on the computer facilities but on some physically relevant parameters (say, dissipation range of wavevectors);
 - ii,b) Most clusters are integrable;
 - ii,c) Ansatz functions for non-integrable clusters can be chosen not due to some computational reasons but according to the intrinsic properties of the physical system defined by the form of its dynamical invariants.
- iii) General mathematical results [4] on resonant clusters are valid for arbitrary Hamiltonian $\mathcal{H}_j, j > 3$, though computation of clusters [5] is more involved then.

Acknowledgements. EK acknowledges the support of the Austrian Science Foundation (FWF) under project P20164-N18 “Discrete resonances in nonlinear wave systems”.

-
- * Electronic address: mig'busta@yahoo.com, lena@risc.uni-linz.ac.at
 - [1] V.E. Zakharov, V.S. L'vov and G. Falkovich. **Kolmogorov Spectra of Turbulence**. Series in Nonlinear Dynamics, Springer (1992)
 - [2] V.E. Zakharov, A.O. Korotkevich, A.N. Pushkarev and A.I. Dyachenko. *JETP Lett.* **82**(8): 491 (2005)
 - [3] E.A. Kartashova. *JETP Lett.* **83**(7): 341 (2006)
 - [4] E.A. Kartashova. **AMS Transl.** **2**, pp. 95-129 (1998)
 - [5] E. Kartashova and A. Kartashov: *Int. J. Mod. Phys. C* **17**(11): 1579 (2006); *Physica A: Stat. Mech. Appl.* **380**: 66 (2007)
 - [6] E. Kartashova and G. Mayrhofer. *Physica A: Stat. Mech. Appl.* **385**: 527 (2007)
 - [7] E. Kartashova, C. Raab, Ch. Feurer, G. Mayrhofer and W. Schreiner. **Extreme Ocean Waves**, pp. 97-128. Eds: E. Pelinovsky and Ch. Harif, Springer (2008)
 - [8] Kartashova E. *Phys. Rev. Lett.* **98**(21): 214502 (2007)
 - [9] E. Kartashova and V.S. L'vov. Submitted to *Europhys. Lett.* E-print: <http://arxiv.org/abs/0801.3374> (2008)
 - [10] M.D. Bustamante and S.A. Hojman. *J. Phys. A: Math. Gen.* **360**: 151 (2003)
 - [11] E.T. Whittaker and G.N. Watson. **A Course in Modern Analysis**, 4th ed. Cambridge, England: Cambridge University Press (1990)
 - [12] E. Kartashova and V.S. L'vov. *Phys. Rev. Lett.* **98**(19): 198501 (2007)
 - [13] E. Kartashova. *Phys. Rev. Lett.* **72**: 2013 (1994)
 - [14] E. Kartashova. *Theor. Math. Phys.* **99**: 675 (1994)